Monitored Incoherency Patterns of Seismic Ground Motion and Dynamic Response of a Long Cable-Stayed Bridge

Vassilios Lekidis, Savvas Papadopoulos, Christos Karakostas, and Anastasios Sextos

Abstract The Evripos bridge in central Greece, connects the island of Evia to the mainland. The cable-stayed section of the bridge is 395 m in length, with a central span of 215 m and side-spans of 90 m each. The deck, 13.5 m in width, is at 40 m above sea-level, suspended by cables from two, 90 m high pylons. A permanent accelerometer special array of 43 sensors was installed on the bridge in 1994 by the Institute of Engineering Seismology and Earthquake Engineering. Two triaxial sensors have been monitoring the free-field (near pier M4) and pier M5 base response on the mainland (Boeotean) coast and two others the respective locations (pier base M6 and free-field near pier M7) on the Euboean coast. Since then the bridge's behavior to seismic excitations has been continuously monitored and investigated. From various earthquake events recorded at the site, it became obvious that the excitation at each of the aforementioned locations differs, with the lowest peak acceleration values observed at site M7 for all three components, independently of magnitude, azimuth and epicentral distance of the earthquake, a fact that can be attributed to local site conditions. In the present research effort, an investigation of the dynamic response of the Evripos bridge due to the asynchronous base excitations along its supports is carried out. Comparisons are made with the conventional design procedure of assuming a common (synchronous) base excitation at all supports and interesting conclusions are drawn regarding the impact of spatially variable ground motion on the seismic response of the particular bridge.

V. Lekidis · C. Karakostas
Earthquake Planning and Protection Organization (EPPO-ITSAK), 5 Agiou Georgiou Str., Patriarchika Pylaias, GR55535 Thessaloniki, Greece

V. Lekidis
e-mail: lekidis@itsak.gr

C. Karakostas
e-mail: christos@itsak.gr

S. Papadopoulos · A. Sextos (✉)
Department of Civil Engineering, Aristotle University of Thessaloniki, Thessaloniki, Greece
e-mail: asextos@civil.auth.gr

S. Papadopoulos
e-mail: savvaspp@civil.auth.gr

M. Papadrakakis et al. (eds.), *Computational Methods in Earthquake Engineering*, Computational Methods in Applied Sciences 30, DOI 10.1007/978-94-007-6573-3_2,

Keywords Asynchronous base excitation (of bridges) · Bridge instrumentation · Bridge dynamic response · Evripos cable-stayed bridge

1 Introduction

During the last decade, time history analyses have become increasingly popular both for design and research purposes, especially for the case of complex and/or important bridges. This trend has significantly improved the analysis rigor and facilitated the consideration of various physical phenomena that were too complicated to be taken into account in the past. One of those issues, is the identification of a realistic, spatially variable earthquake ground motion (SVEGM) which can be used for the excitation of the bridge for design or assessment purposes. As it is well known, this phenomenon may affect the seismic response of long bridges, or of bridges crossing abruptly changing soil profiles; however, its potentially beneficial or detrimental impact on the final bridge performance cannot be easily assessed in advance [1–5].

One major difficulty in assessing the spatially variable patterns of earthquake ground motion is the complex wave reflections, refractions and superpositions that take place as seismic waves travel through inhomogeneous soil media. Different analytical formulations have been proposed in the past, but the inherent multi-parametric nature of wave propagation and soil-structure interaction makes it practically impossible to predict the spatially varying earthquake input along the bridge length in a deterministic manner. Dense seismograph arrays, primarily in Taiwan, Japan and the U.S., have contributed in shedding some light into this problem which can be primarily attributed to four major factors that take place simultaneously, i.e., wave passage effect, the extended source effect, wave scattering and attenuation effect [6]. The operation of these arrays, also led to the development of numerous empirical, semi-empirical and analytical coherency models, fit to represent the decaying signal correlation with distance and frequency.

Despite the significant impact of the aforementioned analytical approaches and experimental evidence, a reliable and simple methodology for the prediction of the effects of asynchronous motion on bridges is still lacking. Even modern seismic codes like Eurocode 8 deal with the problem through either simplified code-based calculations or indirect preventive measures involving larger seating deck lengths [7].

An interesting case for the study of this phenomenon using recorded data is the Evripos cable-stayed bridge, which has been permanently monitored by an accelerometer network since 1994 [8, 9]. A series of minor to moderate intensity seismic events have been recorded by this network, providing a useful set of motions recorded both in the vicinity of the structure and on specific locations on the structure and its foundation. The scope of this study therefore, is to:

- Investigate the impact of spatial variable ground motion by processing specific input motions recorded on site as the bridge, due to its overall length, is sensitive to asynchronous motion.

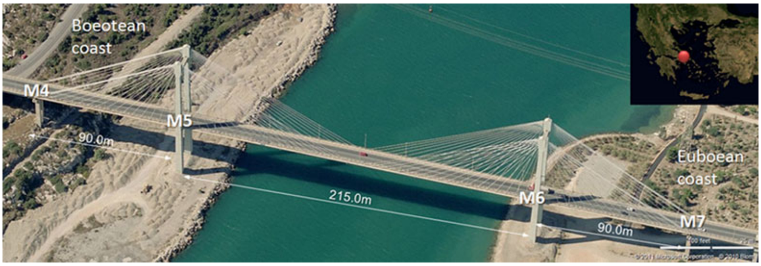

Fig. 1 The central section of the Evripos cable-stayed bridge

- Make use of the recorded data in order to investigate the nature of earthquake ground motion and the effects of its spatial variation on the dynamic response (in terms of forces and displacements) of the particular cable-stayed bridge.

The description of the bridge, its monitoring system as well as its response under various asynchronous ground motion records, is presented in the following.

2 Description of the Evripos Cable-Stayed Bridge

The Evripos bridge, a 694.5 m long R/C structure, connects the Euboean coast in the island of Evia to the Boeotean coast in continental central Greece (Fig. 1). It comprises three parts, i.e. the central cable stayed section and two side (approaching) parts made of pre-stressed R/C beams that rest on elastomeric bearings. The central section of the bridge (Fig. 1) is divided into three spans of length 90 m, 215 m and 90 m respectively, while the deck (of 13.50 m width) is suspended by the 90 m height pylons M5 and M6 with cables. The displacements of the deck along the longitudinal direction are permitted in piers M4 and M7 while those in the transverse direction are blocked [8, 9]. In the present study, it is only the central cable-stayed section that is examined.

As already mentioned, the Evripos cable-stayed bridge behavior is constantly monitored through a special accelerometer array installed by the Institute of Engineering Seismology and Earthquake Engineering (now EPPO-ITSAK). The network is composed by four triaxial accelerometers installed at the base of the bridge, in particular, on the pile caps of piers M5 and M6 and on soil surface in areas adjacent to piers M4 and M7. There are also 31 additional uniaxial accelerometers installed on the superstructure, for system identification purposes. It is noted that all sensors have common time and common trigger settings [8, 9] thus permitting signal processing and correlation. The Finite Element model of the bridge is illustrated in Fig. 2.

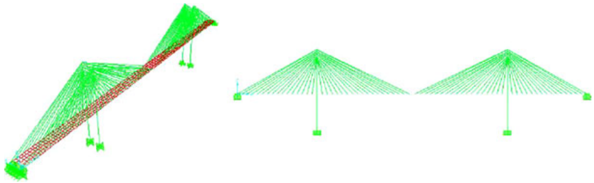

Fig. 2 Finite element model of the Evripos cable-stayed bridge

3 Earthquake Strong Motion Data Available on Site

The expectation that the central cable stayed section of the bridge is asynchronously excited during an earthquake due to its significant overall length (395 m) aroused the interest in processing specific sets of records available on-site so that spatial variation of earthquake ground motion could be confirmed or not. Among the available data of seismic events that have been recorded since the installation of the accelerometers array, the recorded at the base of the piers accelerograms of the Athens earthquake (7/9/1999, M_s) which took place at a source-to-site distance of 43 km were selected and are illustrated in Fig. 3.

Firstly, the time histories were filtered, using a band-pass filter in the frequency range 0.65–25 Hz in order to remove the effects of the inertial soil bridge interaction. In order to measure the similarity of the seismic motions between all pairs of records, it is necessary to compute the lagged coherency, which indicates the degree to which two different accelerograms are related [10], according to the following expression:

$$\left|\overline{\gamma}_{jk}^{M}(\omega)\right| = \frac{|\overline{S}_{jk}^{M}(\omega)|}{\sqrt{\overline{S}_{jj}^{M}(\omega)\overline{S}_{kk}^{M}(\omega)}} \tag{1}$$

where $\overline{S}_{jj}$ and $\overline{S}_{kk}$ are the smoothed power spectral densities at the stations j and k and are given by:

$$\overline{S}_{jj}(\omega_n) = \sum_{m=-M}^{+M} W(m\Delta\omega)S_{jj}(\omega_n + m\Delta\omega) \tag{2}$$

where ω_n is the discrete frequency, $W(m\Delta\omega)$ the (Hamming) spectral window and S_{jj} the unsmoothed power spectra. $\overline{S}_{jk}$ is the smoothed cross spectral densities between the stations j and k expressed as:

$$\overline{S}_{jk}(\omega_n) = \frac{2\pi}{T}\sum_{m=-M}^{+M} W(m\Delta\omega)\Lambda_j(\omega_n + m\Delta\omega)\Lambda_k(\omega_n + m\Delta\omega) \times \exp\left\{i\left[\Phi_k(\omega_n + m\Delta\omega) - \Phi_k(\omega_n + m\Delta\omega)\right]\right\} \tag{3}$$

where Λ_j and Λ_k are the Fourier amplitudes in stations j and k respectively and Φ_j and Φ_k are the corresponding phases. An 11-point Hamming window was used for smoothing as proposed by Abrahamson for 5 % structural damping [10, 11]. The described process was written as a GUI-based, Matlab script.

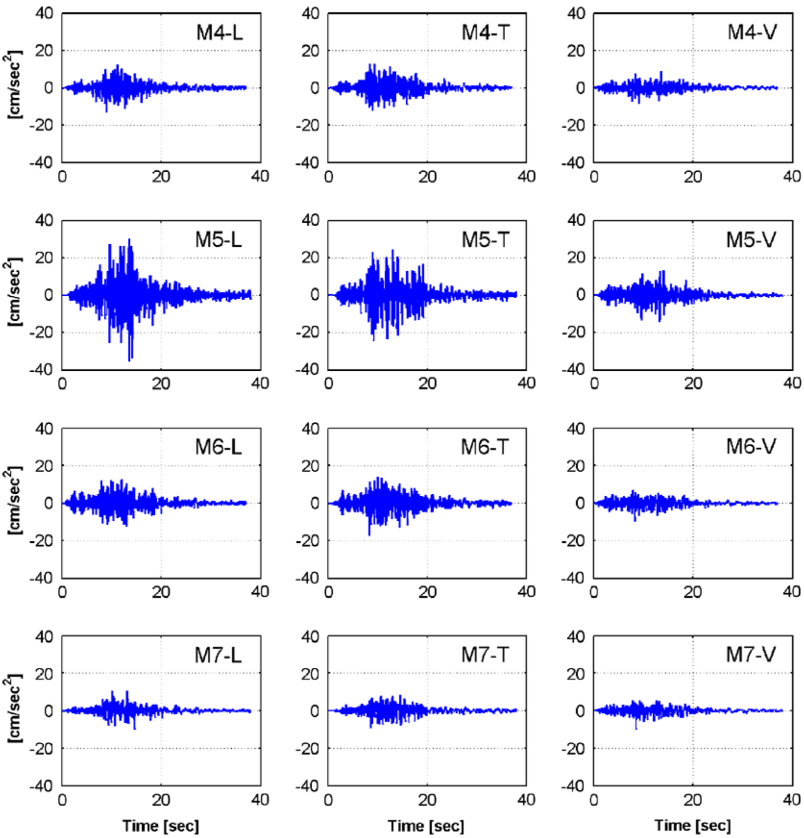

Fig. 3 Horizontal and vertical components of the strong ground motions recorded at the base of piers M4, M5, M6 and M7 due to the 1999 $M_s = 5.9$ Athens earthquake

The diagrams of lagged coherency, computed individually for all components of the records and for all pairs, are illustrated in Fig. 4 and confirm the spatially variable nature of the ground motion. As anticipated, at low frequencies and short separation distances the lagged coherency tends to unity while it decreases with increasing separation distance and frequency.

In order for the seismic motion to be able to be predicted at different stations over an extended area, several parametric coherency models have been proposed in the literature. Many of them are empirical models developed with regression fitting of different functional forms on specific data; some others are semi-empirical models the functional form of which developed with analytical procedures but their parameters were evaluated by recorded data; lastly there are also some analytical models [10].

The comparison of the computed incoherences with one of the empirical and a semi-empirical coherency model for the pairs M4-M5, M4-M6 and M4-M7 in horizontal directions is made in Fig. 5. The models used for this comparison are: the single functional form for the horizontal coherency of Abrahamson [6]:

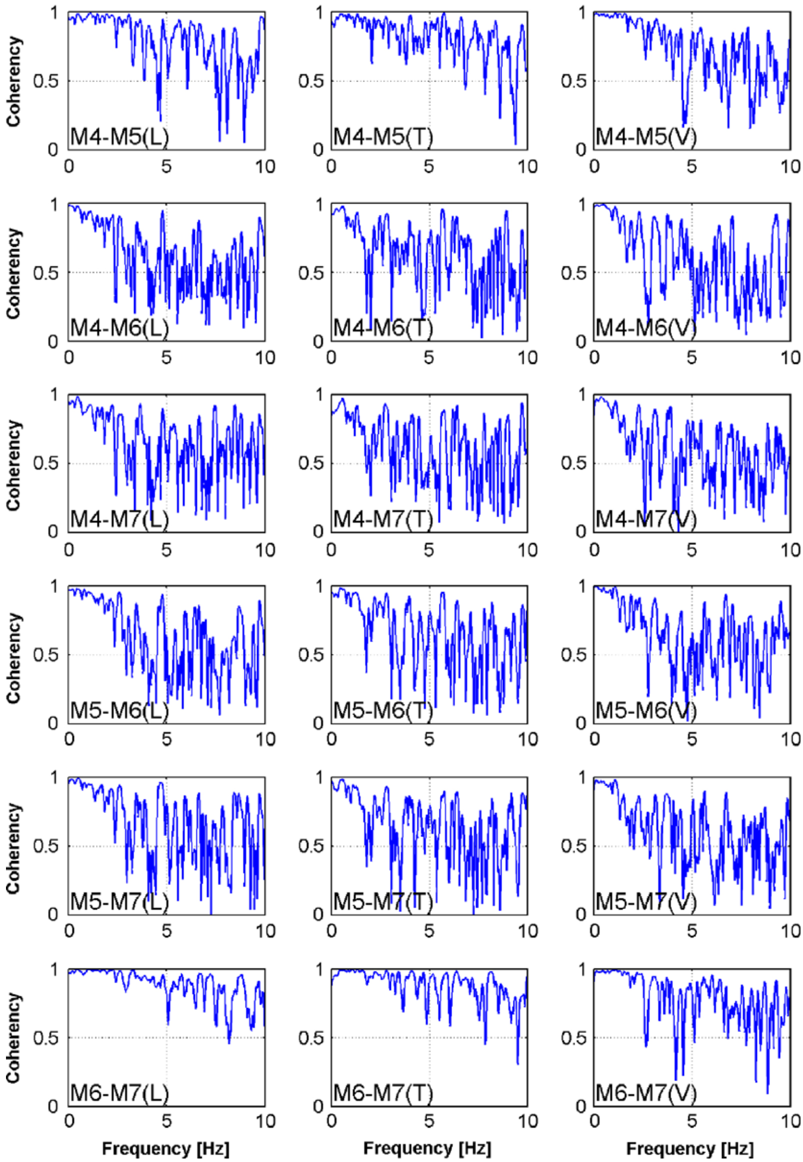

Fig. 4 Lagged coherency of motions between piers M4-M5 (90 m), M4-M6 (305 m), M4-M7 (395 m), M5-M6 (215 m), M5-M7 (90 m) and M6-M7 (90 m)

$$\left|\gamma^{H}(\xi, f)\right| = \tanh\left\{\frac{c_1^H(\xi)}{1 + c_2^H(\xi) f + c_4^H(\xi) f^2} + \left(4.80 - c_1^H(\xi)\right)\exp\left[c_2^H(\xi) f\right] + 0.35\right\} \quad (4)$$

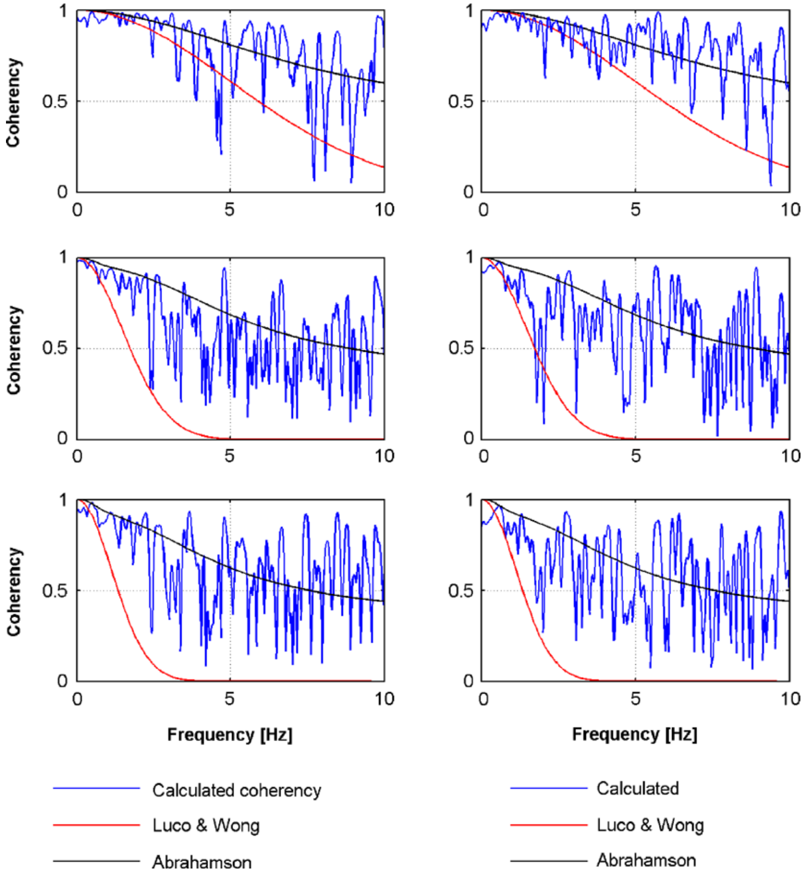

Fig. 5 Comparison between observed and predicted coherency loss for different empirical and semi-empirical models

where:

$$\begin{aligned}
c_1^H(\xi) &= \frac{3.95}{1 + 0.0077\xi + 0.000023\xi^2} + 0.85\exp[-0.00013\xi] \\
c_2^H(\xi) &= \frac{0.4[1 - (1 + (\xi/5)^3)^{-1}]}{[1 + (\xi/190)^8][1 + (\xi/180)^3]} \\
c_3^H(\xi) &= 3\exp\big([-0.05\xi] - 1\big) - 0.0018\xi \\
c_4^H(\xi) &= -0.598 + 0.106\ln(\xi + 325) - 0.0151\exp[-0.6\xi]
\end{aligned} \tag{5}$$

and the most commonly used pattern proposed by Luco and Wong which has the form [12]:

$$\left|\gamma(\xi,\omega)\right| = e^{-\left(\frac{v\omega\xi}{V_s}\right)} = e^{-a^2\omega^2\xi^2} \tag{6}$$

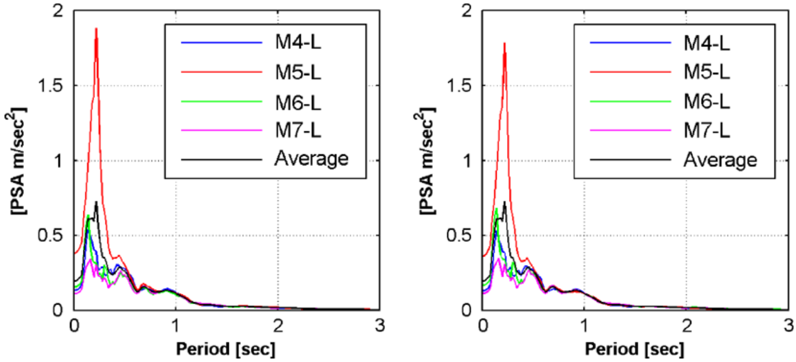

Fig. 6 5 % damped elastic response spectra of the longitudinal components of the records at piers M4-M7 compared to the scaled ones (on the *right*) at the average spectrum for $T = 1.64$ sec

where the coherency drop parameter α controls the exponential decay and ξ is the distance between two stations examined. The drop parameter is usually taken equal to $2.5 \cdot 10^{-4}$ sec/m, but in this specific case, the results are not satisfactory. On the other hand, the model of Abrahamson can predict the loss of coherency much better than Luco and Wong as illustrated in Fig. 5.

4 Analyses Performed

Most analytical or numerical studies investigating the effects of spatial variability of earthquake ground motion on the response of bridges compare the results of multiple-support excitation analysis with those of a reference condition which typically assumes synchronous excitation among all bridge supports. The comparison can then be made in terms of a ratio of the action effects (forces or displacements) of specific structural components over the response under synchronous conditions.

In the case examined herein though, the fact that the ground motions have been recorded at the bases of the four bridge piers gives the actual asynchronous excitations due to the existing seismo-tectonic and soil conditions of the site under study, but at the same time makes it difficult to the corresponding compatible "synchronous" excitation conditions. One option would have been to select one of the recorded motions and apply it synchronously at all pier supports; however, this option is limited by the fact that the available records show significant discrepancy in terms of both their PGA and spectral amplification, primarily due to local site effects at the location of pier M5 (Fig. 6).

In order to overcome this difficulty, it was decided to adopt the following procedure: strongest component of the motions recorded is in the longitudinal direction, all records (in all components) are scaled (Table 1) to the average spectral acceleration of all records at period $T = 1.64$ sec, which is the period of the highest contributing mode, activating 76 % of the mass in the longitudinal direction (Table 2).

Table 1 The scaling factors for the records at M4, M5, M6, M7 compared to the average response spectrum for $T = 1.64$ sec

Pier	M4	M5	M6	M7
Scale factor	0.977	0.947	1.069	1.014

Table 2 Dynamic characteristics (eigenfrequencies and corresponding modal contribution) of the Evripos cable-stayed bridge

Mode ID	Period	UX	UY	UZ	RX	RY	RZ
#1	2.712	0	0	6.7	1.2	2.3	0
#2	2.385	20.2	0	0	0	0	0
#3	2.061	0	58.3	0	3.4	0	47.2
#4	1.645	76.3	0	0	0	0	0
#5	1.298	0	0	6.2	1.4	5.5	0
#9	1.065	0	0	37.4	7.3	28.8	0

Then, four different "synchronous" excitation scenarios are developed, assuming each time that the scaled motions in piers M4, M5, M6 and M7 respectively, are applied uniformly at all supports. Given the aforementioned scaling, it is deemed that the four different versions of uniform excitation are compatible in terms of spectral amplification (at least at the period of vibration that is affected by the dominant earthquake component), while the fact that all the resulting scaling factors are close to unity, guarantees that the scaling-induced dispersion is limited.

Based on the above, five non-linear dynamic analyses of the Evripos cable-stayed bridge are performed using the computer program SAP2000, i.e. one using the recorded set of asynchronous motions and four considering the aforementioned compatible "synchronous" excitation scenarios. All three components of the excitations were applied simultaneously. The geometrical non-linearity induced by the bridge cables was considered assuming tension-only capabilities and the initial cable stress state due to dead loading was applied through non-linear staged-construction static analysis.

Beam elements were used to model the piers, while the bridge deck was modeled by shell elements. Piers were assumed fixed at their bases, while the supporting conditions at the two bridge edges were considered as rollers in the longitudinal direction and pined in the transverse.

The amplitude of the seismic moments (i.e., the earthquake-induced bending moments at the bases of piers M4 and M7 and at one of the two columns at each pier M5 and M6), the displacements at the top of each pier and the displacements at the middle of the deck are examined for all asynchronous and synchronous excitation cases previously presented.

Figure 7 presents the comparison between the computed seismic moments at the base of pier M6 using the Athens 1999 (asynchronous) recorded motions, and

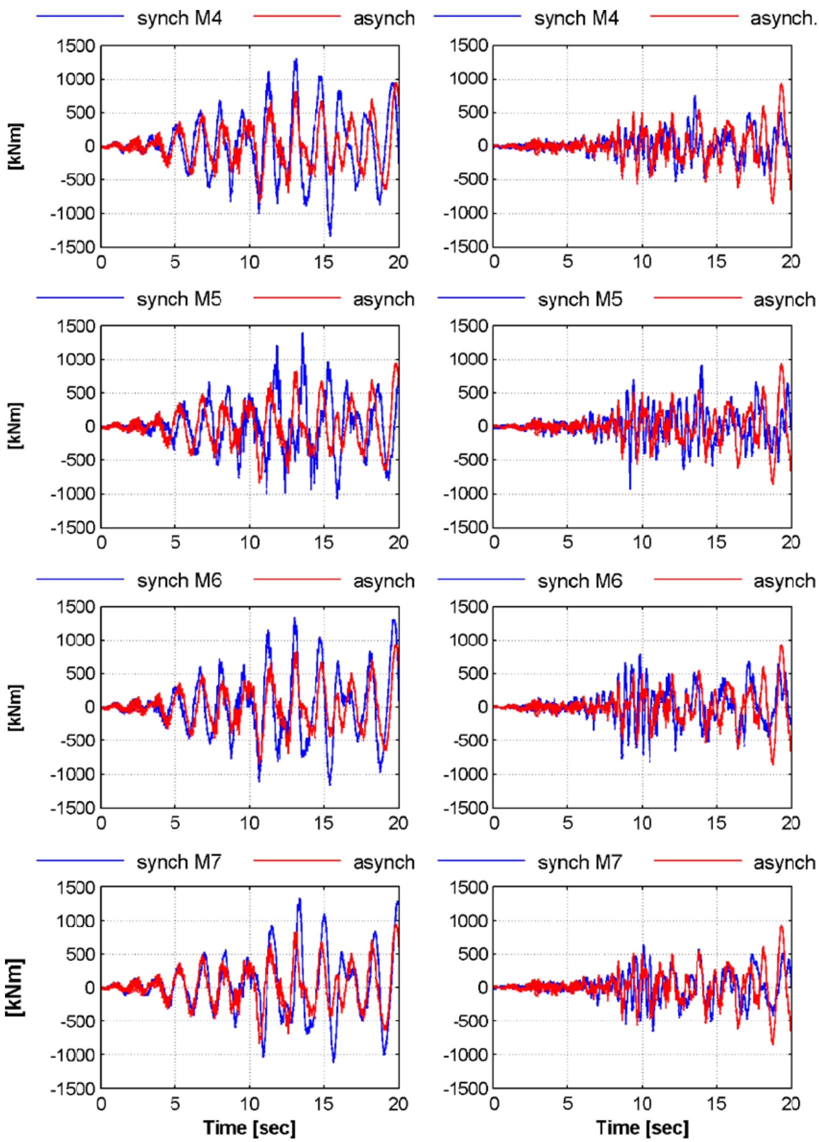

Fig. 7 Comparison of the computed seismic moments at the base of pier M6 using the Athens 1999 (asynchronous) recorded motions, with those computed through the four "synchronous" excitation scenarios (uniform application of records M4, M5, M6, M7). On the *left* the moment vector M2 is parallel to the bridge (transverse bending) while on the *right* it is normal to the bridge (M3, longitudinal bending)

those computed through the four "synchronous" excitation scenarios, that is, by the uniform application of records M4, M5, M6, and M7 respectively. The comparison of the maxima among all cases are summarized in Table 3.

Table 3 Comparison of maximum absolute earthquake induced bending moments developed in pier M6 for synchronous and asynchronous excitation (cases M4, M5, M6, M7)

Uniform excitation scenario	Case studied	Pier M5		Pier M6	
		M2 [kNm]	M3 [kNm]	M2 [kNm]	M3 [kNm]
Synch M4	Synch	1350.70	798.54	1338.30	759.11
	Asynch	833.53	743.05	949.48	943.70
	Asynch/Synch-1	−38 %	−7 %	−29 %	+24 %
Synch M5	Synch	1510.39	1008.53	1403.31	919.10
	Asynch	833.53	743.05	949.48	943.70
	Asynch/Synch-1	−45 %	−26 %	−32 %	+3 %
Synch M6	Synch	1401.33	981.36	1345.28	815.00
	Asynch	833.53	743.05	949.48	943.70
	Asynch/Synch-1	−41 %	−24 %	−29 %	+16 %
Synch M7	Synch	1314.49	849.06	1335.77	658.05
	Asynch	833.53	743.05	949.48	943.70
	Asynch/Synch-1	−37 %	−13 %	−29 %	+43 %

It can be seen that the moments M_2 developed at the base of pier M6 transversely to the bridge plane, due to the asynchronous recorded ground motions is systematically lower regardless of the "synchronous" excitation pattern adopted. As anticipated, this is more intense (approximately 32 %) for the synchronous case involving the uniform application of record M5, which, despite of the scaling to a common level of spectral amplification, still corresponds to the highest PGA among the records at all locations. On the other hand, the situation reverses for the bending moments M_3 within the bridge plane and the asynchronous excitation results in higher levels of stress in all cases, reaching 43 % increase in the extreme case of applying record M7 uniformly at all support points. The respective results for pier M5 are also summarized in Table 3. It can be seen that seismically-induced bending moments in both directions are decreased when assuming non-uniform excitation conditions independently of the scenario adopted.

As far as the displacements are concerned, the corresponding time histories are plotted in Fig. 8 and Fig. 9 for the top of pylons M5 and M6 respectively, while the maximum in time displacements for all directions are compared in Table 4 and Table 5. The respective magnitudes at the middle of the deck are summarized in Table 6. More specifically, asynchronous excitation is systematically favorable for the span middle deck displacements which are decreased up to 36 %, 45 % and 63 % along the three principal directions U_x, U_y and U_z.

The same trend is also observed for the case of the top of pylon M5—though to a lesser degree—and with the exception of a minor (6 %) increase in longitudinal displacements for one of the scenarios studied. In contrast to the above, the transverse displacements at the top of pylon M6 derived under the asynchronous

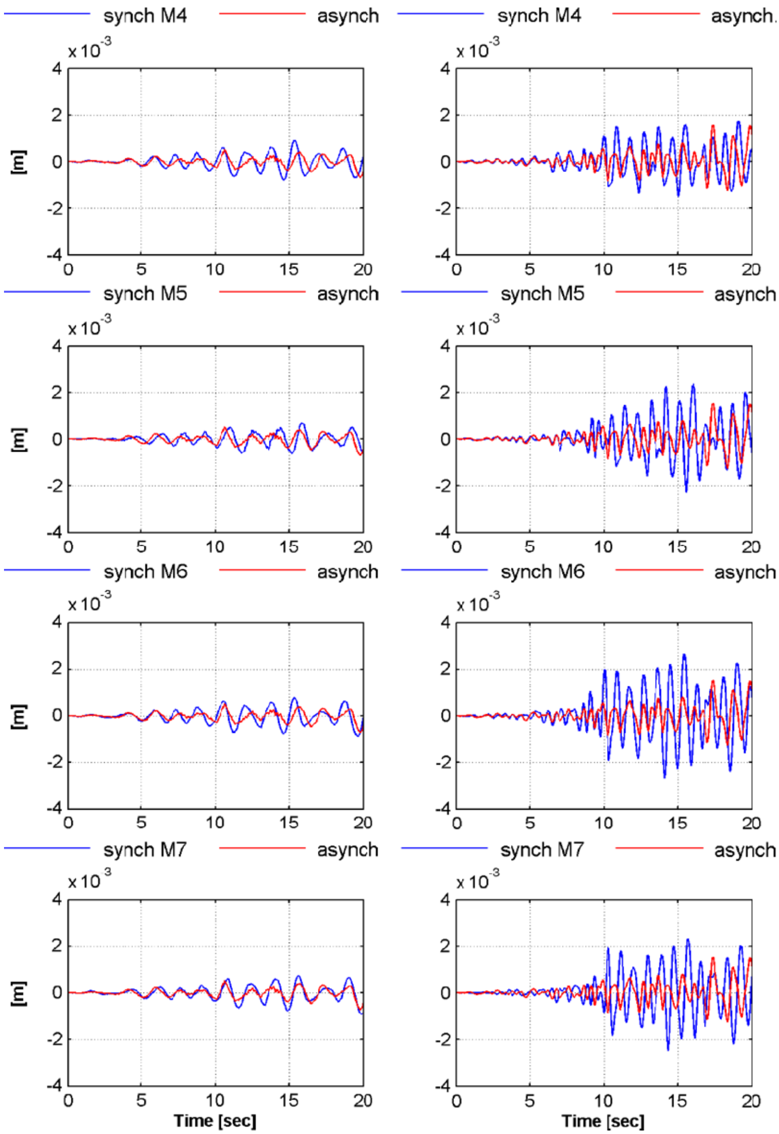

Fig. 8 Comparison of the seismic displacements at the top of pylon M5 using the Athens 1999 (asynchronous) recorded motions, with those computed through the four "synchronous" excitation scenarios (uniform application of records M4, M5, M6, M7). On the *left* displacements are in the longitudinal bridge direction while on the *right* are in transverse direction

recorded ground motions are increased compared to the synchronous case and are almost double (increased by 82 %) when compared to the uniform application of record M4. As for the vertical displacements in both pylons can either decrease or increase depending on the assumed "synchronous" scenario.

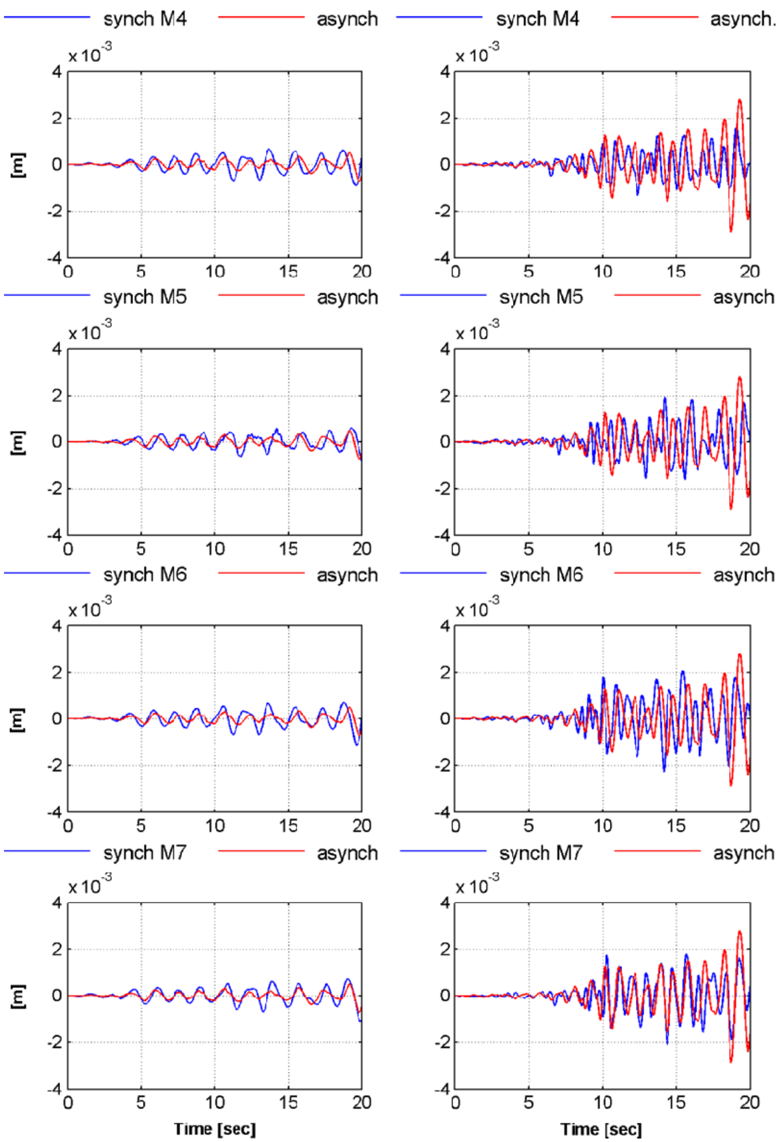

Fig. 9 Comparison of the seismic displacements at the top of pylon M6 using the Athens 1999 (asynchronous) recorded motions, with those computed through the four "synchronous" excitation scenarios (uniform application of records M4, M5, M6, M7). On the *left* displacements are in the longitudinal bridge direction while on the *right* are in the transverse direction

These results indicate that the inherently complex nature of ground motion incoherency is strongly correlated to the dynamic characteristics of the excited structure and does not systematically lead to a uniform increase or decrease of the corresponding action effects.

Table 4 Comparison of maximum absolute earthquake induced displacements [cm] developed at top of pier M5 for synchronous and asynchronous excitation (cases M4, M5, M6, M7)

Uniform excitation scenario	Case studied	U_x [cm]	U_y [cm]	U_z [cm]
Synch M4	Synch	0.09	0.18	0.05
	Asynch	0.07	0.16	0.05
	Asynch/Synch-1	−22 %	−12 %	+7 %
Synch M5	Synch	0.067	0.23	0.05
	Asynch	0.071	0.16	0.05
	Asynch/Synch-1	+6 %	−34 %	0 %
Synch M6	Synch	0.09	0.27	0.06
	Asynch	0.07	0.16	0.05
	Asynch/Synch-1	−20 %	−42 %	−14 %
Synch M7	Synch	0.09	0.25	0.05
	Asynch	0.07	0.16	0.05
	Asynch/Synch-1	−23 %	−37 %	−6 %

Table 5 Comparison of maximum absolute earthquake induced displacements [cm] developed at top of pier M6 for synchronous and asynchronous excitation (cases M4, M5, M6, M7)

Uniform excitation scenario	Case studied	U_x [cm]	U_y [cm]	U_z [cm]
Synch M4	Synch	0.09	0.16	0.04
	Asynch	0.07	0.29	0.05
	Asynch/Synch-1	−20 %	+82 %	+11 %
Synch M5	Synch	0.08	0.19	0.047
	Asynch	0.07	0.29	0.049
	Asynch/Synch-1	−10 %	+49 %	+4 %
Synch M6	Synch	0.11	0.23	0.054
	Asynch	0.07	0.29	0.049
	Asynch/Synch-1	−36 %	+28 %	−9 %
Synch M7	Synch	0.11	0.21	0.050
	Asynch	0.07	0.29	0.049
	Asynch/Synch-1	−35 %	+38 %	−2 %

Table 6 Comparison of maximum absolute earthquake induced displacements [cm] developed at the middle of the bridge deck for synchronous and asynchronous excitation (cases M4, M5, M6, M7)

Uniform excitation scenario	Case studied	U_x [cm]	U_y [cm]	U_z [cm]
Synch M4	Synch	0.11	0.14	0.16
	Asynch	0.08	0.10	0.07
	Asynch/Synch-1	−28 %	−25 %	−56 %
Synch M5	Synch	0.09	0.14	0.17
	Asynch	0.08	0.10	0.07
	Asynch/Synch-1	−15 %	−29 %	−58 %
Synch M6	Synch	0.12	0.18	0.20
	Asynch	0.08	0.10	0.07
	Asynch/Synch-1	−36 %	−45 %	−63 %
Synch M7	Synch	0.12	0.16	0.18
	Asynch	0.08	0.10	0.07
	Asynch/Synch-1	−36 %	−41 %	−60 %

5 Conclusions

The scope of this study was to examine the effects of asynchronous excitation on the Evripos cable-stayed bridge, utilizing the recorded time histories at four locations of the accelerometer network maintained by EPPO-ITSAK, due to the $M_s = 5.9$, 7/9/1999 Athens earthquake. Initially the records were filtered to remove inertial interaction effects and after that their coherency was computed for all available record pairs. Comparison of these results with two different coherency models presented in literature proved that there was a significant difference in the accuracy of the predictions of the two models, and hence the selection of a coherency model for the investigation of spatial variability of earthquake ground motion should be done with caution. A detailed finite element model of the cable-stayed bridge was developed and its response was computed using both the recorded motions and four synchronous excitation scenarios. The comparative study of the results indicates that:

- For the particular bridge studied, spatial variability of seismic ground motion has a generally favorable effect, at least on the pier base bending moments and the displacements middle of the central span deck. Apparently, the extent of this beneficial phenomenon is very much dependent on the assumptions made regarding the definition of the "synchronous" excitation, which, in contrast to the actual, recorded asynchronous case, is not obvious.

- There are specific cases (i.e., out-of-plane bending moments and displacements at the top of the two bridge pylons) where the asynchronous excitation has a clearly critical effect.

The results of the investigations of the present study indicate that the complex nature of ground motion incoherency is strongly correlated to the dynamic characteristics of the excited structure and does not systematically lead to a uniform increase or decrease of the corresponding action effects.

References

1. Burdette NJ, Elnashai AS (2008) Effect of asynchronous earthquake motion on complex bridges. II: Results and implications on assessment. J Bridge Eng 13:166–172
2. Deodatis G, Saxena V, Shinozuka M (2000) Effects of spatial variability of ground motion on bridge fragility curves. In: Eighth ASCE specialty conference on probabilistic mechanics and structural reliability
3. Lupoi A, Franchin P, Pinto PE, Monti G (2005) Seismic design of bridges accounting for spatial variability of ground motion. Earthq Eng Struct Dyn 34:327–348. doi:10.1002/eqe.444
4. Nazmy AS, Abdel-Ghaffar AM (1992) Effects of ground motion spatial variability on the response of cable-stayed bridges. Earthq Eng Struct Dyn 21:1–20. doi:10.1002/eqe.4290210101
5. Sextos AG, Kappos AJ, Pitilakis KD (2003) Inelastic dynamic analysis of RC bridges accounting for spatial variability of ground motion, site effects and soil-structure interaction phenomena. Part 2: Parametric study. Earthq Eng Struct Dyn 32:629–652. doi:10.1002/eqe.242
6. Abrahamson NA (1993) Spatial variation of multiple support inputs. In: Proceedings of the 1st US seminar on seismic evaluation and retrofit of steel bridges. A Caltrans and University of California at Berkeley seminar
7. Sextos AG, Kappos AJ (2008) Evaluation of seismic response of bridges under asynchronous excitation and comparisons with Eurocode 8-2 provisions. Bull Earthq Eng 7:519–545. doi:10.1007/s10518-008-9090-5
8. Lekidis V, Tsakiri M, Makra K, Karakostas C, Klimis N, Sous I (2005) Evaluation of dynamic response and local soil effects of the Evripos cable-stayed bridge using multi-sensor monitoring systems. Eng Geol 79:43–59. doi:10.1016/j.enggeo.2004.10.015
9. Lekidis V (2003) Investigation of the seismic response of the Evripos high bridge: experimental and analytical approach. Thessaloniki
10. Zerva A (2009) Spatial Variation of Seismic Ground Motions: Modeling and Engineering Applications. CRC Press, Boca Raton
11. Abrahamson NA, Schneider JF, Stepp JC (1991) Empirical spatial coherency functions for applications to soil-structure interaction analyses. Earthq Spectra 7:1–28
12. Luco JE, Wong HL (1986) Response of a rigid foundation to a spatially random ground motion. Earthq Eng Struct Dyn 14:891–908. doi:10.1002/eqe.4290140606

Springer

http://www.springer.com/978-94-007-6572-6

Computational Methods in Earthquake Engineering
Volume 2
Papadrakakis, M.; Fragiadakis, M.; Plevris, V. (Eds.)
2013, XV, 636 p., Hardcover
ISBN: 978-94-007-6572-6